

FIELD PERFORMANCE
Falling Weight Deflectometer Data
Analysis

Recycled Asphalt Pavement and
Recycled Concrete Aggregate

TPF-5 (129) Recycled Unbound Materials

Mn/DOT Contract No. 89264 Work Order No. 2

CFMS Contract No. B14513

Task IIBa: Field Performance and Maintenance: FWD Survey

Gregory J. Schaertl, Tuncer B. Edil, and Craig H. Benson

University of Wisconsin- Madison

August 21, 2010

INTRODUCTION

The objectives of this study were (1) to determine the maximum deflection of each pavement section under simulated loading by the FWD and (2) to determine the resilient modulus of the pavement layers, focusing on the performance of base course layers composed of recycled asphalt pavement (RAP), recycled concrete aggregate (RCA) and a 50-50 blend of RCA with conventional base course aggregate (Class 5). RAP refers the removal and reuse of the hot mix asphalt (HMA) layer of an existing roadway, and RCA refers to the reuse of materials reclaimed from roadways as well as from other structures such as old buildings and airport runways. A conventional base course meeting the gradation standard of a Minnesota Department of Transportation Class 5 aggregate was used as a reference material in this study.

MATERIALS AND METHODS

Index properties and compaction data for RAP, RCA, blended RCA/Class 5, and Class 5 are presented in Table 1, with particle size distribution graphs presented in Fig. 1. Each of the four materials is classified as non-plastic, poorly graded gravel, with the RAP specimen having an asphalt content of 4.8%.

Table 1. Index properties for RAP, RCA, Blended RCA/Class 5, and Class 5.

Sample	W_{opt} (%)	$\gamma_{d max}$ (kN/m ³)	LL (%)	PL (%)	Gravel Content (%)	Sand Content (%)	Fine Content (%)	USCS Symbol
RAP	6.7	20.8	NP	NP	31.8	67.4	0.8	SP
RCA	11.2	19.5	NP	NP	31.8	64.9	3.3	SP
Blend	8.9	20.1	NP	NP	32.7	63.9	3.4	SP
Class 5	8.0	20.7	NP	NP	28.1	64.2	7.7	SP

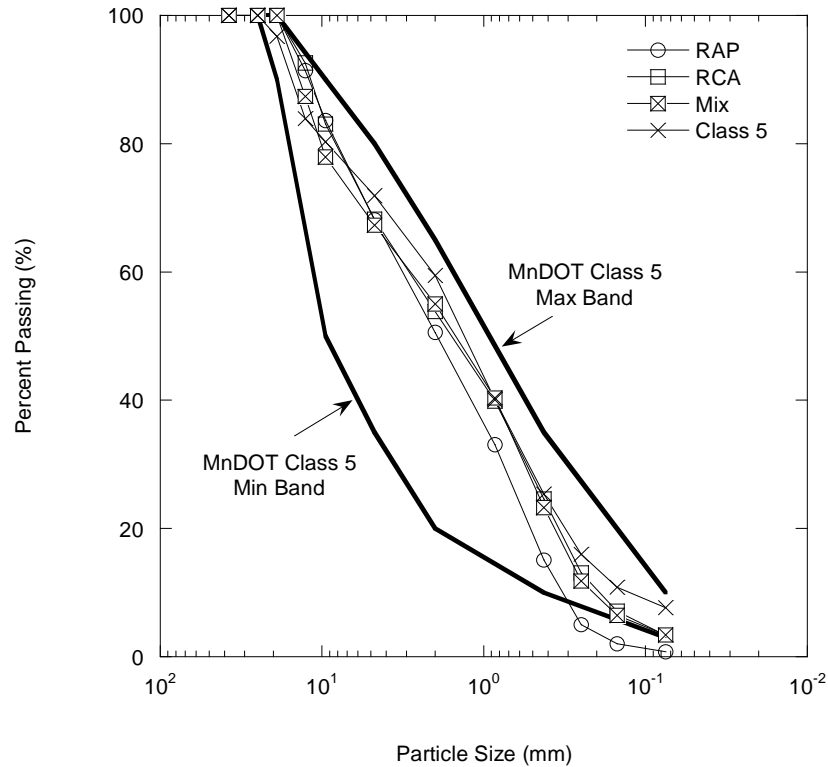


Fig.1. Particle size distributions for RAP, RCA, Blended RCA/Class 5 and Class 5 with MnDOT specifications.

Field-scale in-situ moduli of the materials were obtained from Falling Weight Deflectometer (FWD) tests performed at the MnROAD testing facility near Albertville, Minnesota. Traffic is diverted from westbound I-94 and onto the MnROAD mainline, which is 3.5 miles long by 2 lanes wide. Four test cells were constructed for each of the four base materials tested; the pavement profiles are shown in Fig.2. FWD analysis is performed on different dates throughout the year, and the modulus of each base course can be determined over time.

Cell 16: Recycled Concrete Aggregate (RCA)	Cell 17: Blended 50% / 50% RCA/Class 5 (Blend)	Cell 18: Recycled Asphalt Pavement (RAP)	Cell 19: Mn/DOT Class 5 Aggregate (Class 5)
127 mm Asphalt Concrete	127 mm Asphalt Concrete	127 mm Asphalt Concrete	127 mm Asphalt Concrete
305 mm RCA	305 mm Blend	305 mm RAP	305 mm Class 5
305 mm Class 3 Aggregate	305 mm Class 3 Aggregate	305 mm Class 3 Aggregate	305 mm Class 3 Aggregate
178 mm Select Granular Material	178 mm Select Granular Material	178 mm Select Granular Material	178 mm Select Granular Material
Clay	Clay	Clay	Clay

Fig. 2. Pavement profiles of cells tested using FWD at MnROAD testing facility. (Adapted from Johnson et al. 2009)

Testing was performed using a trailer-mounted Dynatest model 1000 FWD. The FWD was controlled by an on-site computer that recorded and stored load and deflection data. A 40 kN load was applied by the FWD to a 300-mm-diameter plate in contact with the pavement surface. Surface deflections were measured by nine load transducers located at distances of 0, 0.30, 0.61, 0.91, 1.22, 1.52, and 1.83 meters from the center of the load. FWD tests at each cell were conducted at 200 feet intervals along the mainline alignment, as well as at lateral intervals corresponding to the mid-lane and outer-wheel paths of both the driving and passing lanes.

The measured deflections were used to back-calculate the elastic modulus of the pavement layers using the MODULUS program developed at the Texas Transportation Institute. MODULUS uses linear-elastic theory to back-calculate elastic moduli from FWD data. The back-calculation was based on a four-layer model consisting of asphalt concrete, base course, sub-base and subgrade layers. For the purposes of this analysis, the Class 3 aggregate and select granular material indicated in Fig. 2 were combined as one layer. The Pavement profile and deflection data were provided by the Minnesota Department of Transportation (Mn/DOT). The asphalt surface, base course, and sub-base layers were assigned a Poisson's ratio of 0.35, and the subgrade layer was assigned a Poisson's ratio of 0.40 (Huang 2004).

RESULTS AND DISCUSSION

Maximum Deflection of Test Cells

The average maximum elastic deflection and 1-standard deviation of all tests at a given time experienced by each of the four test cells is presented in Fig.3 as a function of time. As the air temperature warms during spring 2009, the gradual increase in deflection can be attributed to an increase in viscosity in the HMA layer and a gradual thawing of the subgrade and subbase layers. The maximum deflection occurs during summer 2009 when air temperature is highest and HMA viscosity is the greatest. The deflection gradually decreases through the fall season as the air temperature drops and the viscosity of the HMA decreases. The deflection recorded during February 2010 is less than 0.1 mm for all test cells, and most likely reflects frozen conditions at the time of testing. Warming temperatures cause the deflection to once again increase during spring 2010 to levels that are comparable in magnitude to deflections experienced during the same time period in 2009.

Overall, Class 5 experienced the greatest elastic maximum deflections, followed by blended RCA/Class 5, RAP, and RCA, respectively. Similar results were reported for small-scale and large-scale tests performed on the same materials by Schaertl (2010) and Son (2010), respectively.

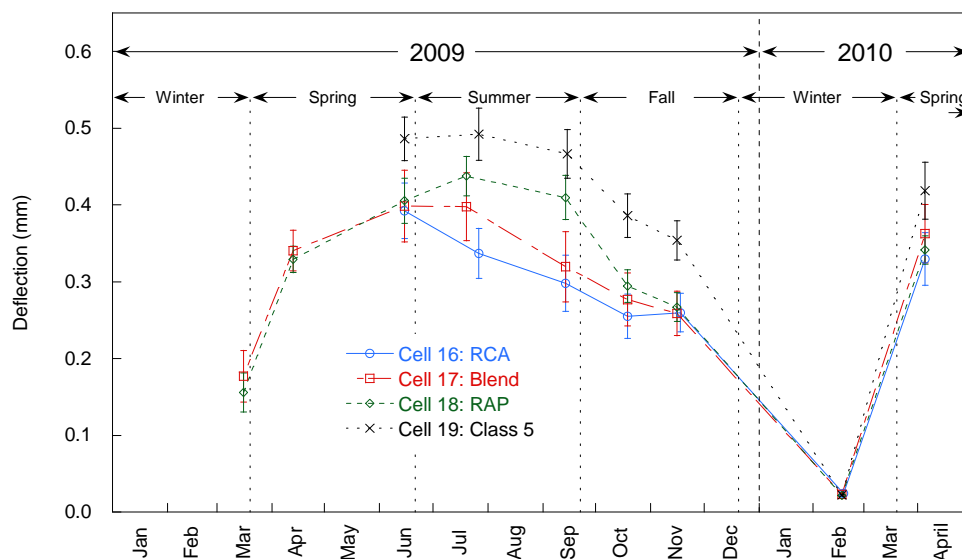


Fig.3. Average center deflection as a function of time for test cells constructed with RAP, RCA, blended RCA/Class 5, and Class 5 base course (error bars represent one standard deviation).

Resilient Modulus of All Layers

The average resilient moduli of the HMA, base course, subbase and subgrade layers for each of the four test cells is presented in Fig.4 as a function of time. The error

bars represent 1-standard deviation of the resilient modulus data for the given layer and time. The broken line between November 2009 and April 2010 represents a non-continuous transition through a frost-penetration period. Modulus 6.0 was not able to analyze deflection data recorded during March 2009 and February 2010 due to very small deflections recorded, most likely due to frozen conditions. The magnitude of the resilient modulus experienced by the HMA is inversely proportional to the air temperature, gradually decreasing from spring to summer, and gradually increasing from summer to fall. The increased viscosity allows the layer to deflect to a greater degree, resulting in a decrease in stiffness. The base, subbase, and subgrade are not as sensitive to temperature and therefore the resilient moduli of these layers remain relatively constant compared to that of the HMA.

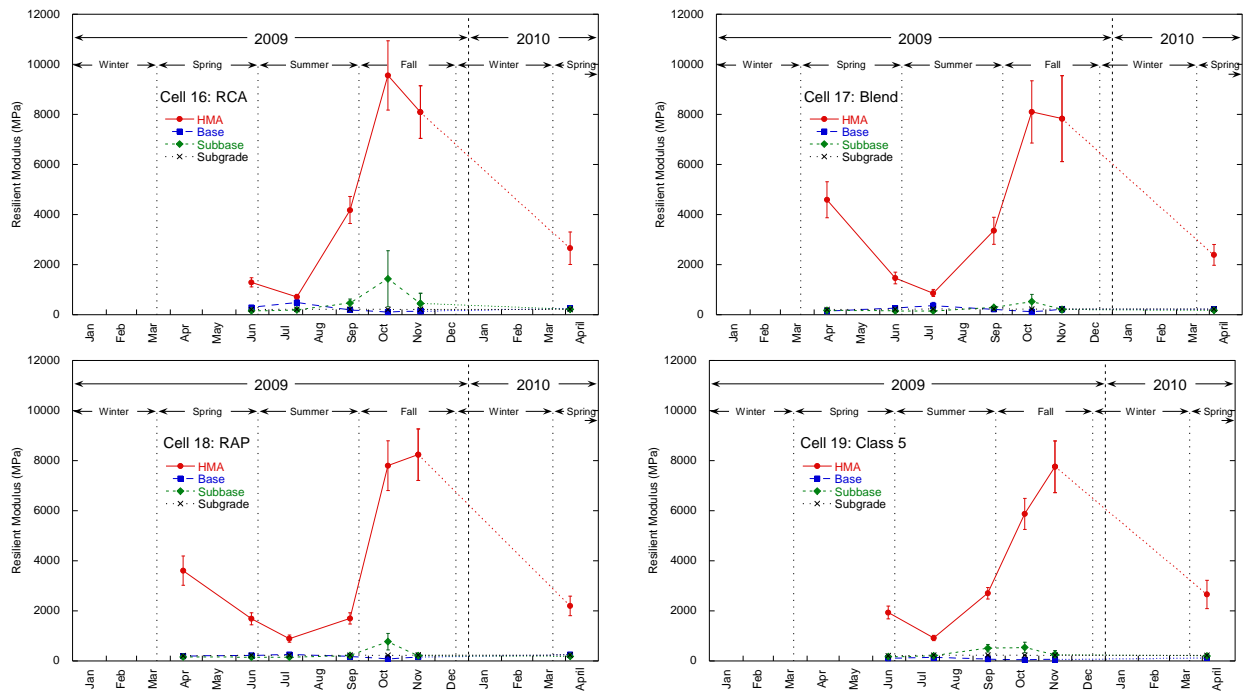


Fig.4. Resilient modulus of HMA, base course, subbase and subgrade as a function of time for test cells constructed with (a) RCA, (b) blended RCA/Class 5, (c) RAP, and (d) Class 5 base course.

Resilient Modulus of Base Course Layers

The resilient modulus of the base course at the midlane and outer wheel paths of both the driving and passing lanes for the four test cells is presented in Fig.5 as a function of time. The data points represent the average of the resilient moduli calculated along each of the measurement alignments. The dotted line connecting November 2009 to April 2010 represents a non-continuous transition through a frost-penetration period. The resilient modulus was greater at the midlane compared to the outer wheel path. The outer wheel path of both lanes encounters a greater amount of wheel loading, and as a consequence experiences a greater degree of compaction. The increased compaction contributes to a denser particle matrix which increases the

overall stiffness of the material. The trend of the base course resilient modulus over time is the opposite of the trend of the HMA: the base course resilient modulus increases with a decrease in HMA modulus, and the decreases with an increase in HMA modulus. As the HMA becomes stiffer, the underlying base course is exposed to less translated stress and, as a result, less strain.

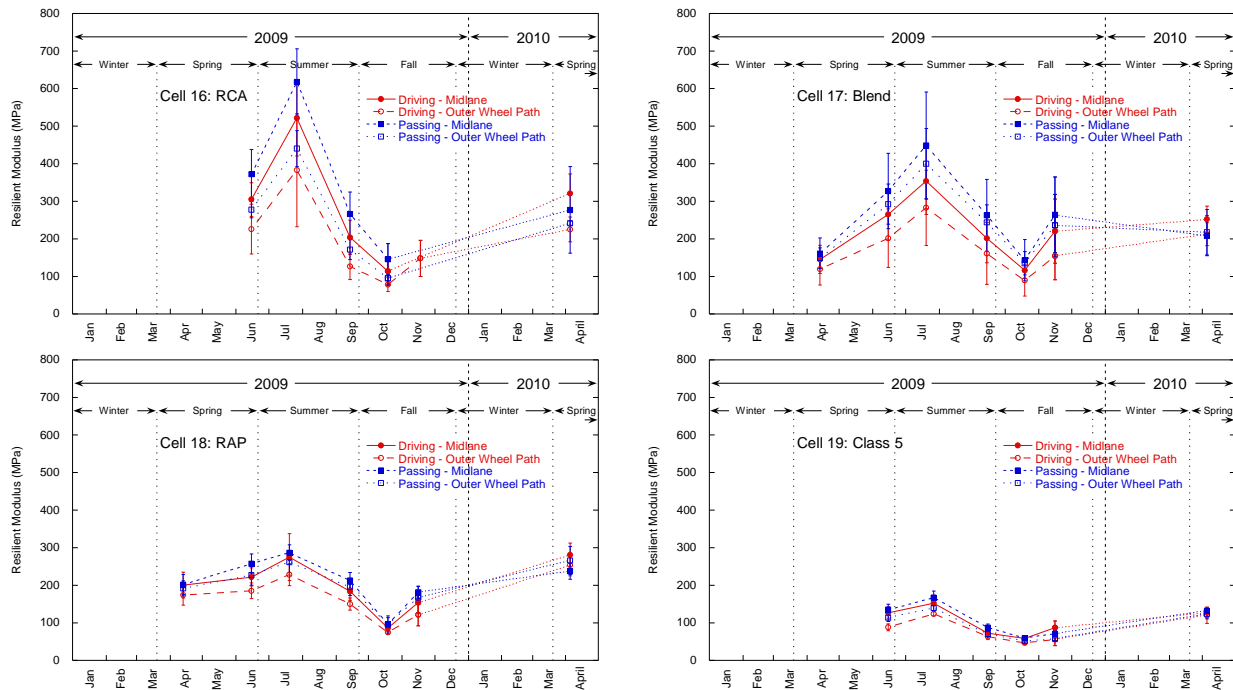


Fig.5. Resilient modulus of base course at the mid-lane and outer-wheel paths of the driving and passing lanes as a function of time for test cells constructed with (a) RCA, (b) blended RCA/Class 5, (c) RAP, and (d) Class 5 base course.

The resilient modulus of the base course at each cell is presented in Fig.6 as a function of time. The resilient modulus from all FWD tests conducted at each cell (varying spatially and temporally) is presented as a box plot in Fig.7. Class 5 had the lowest resilient modulus of the four base course materials tested. Although there was a significant amount of overlap, RCA had the greatest resilient modulus, with blended RCA/Class 5 and RAP having resilient moduli that were comparable in magnitude. The relationship between the magnitudes of the four materials are consistent with the results of small and large-scale laboratory testing conducted by Son (2010) and Schaertl (2010).

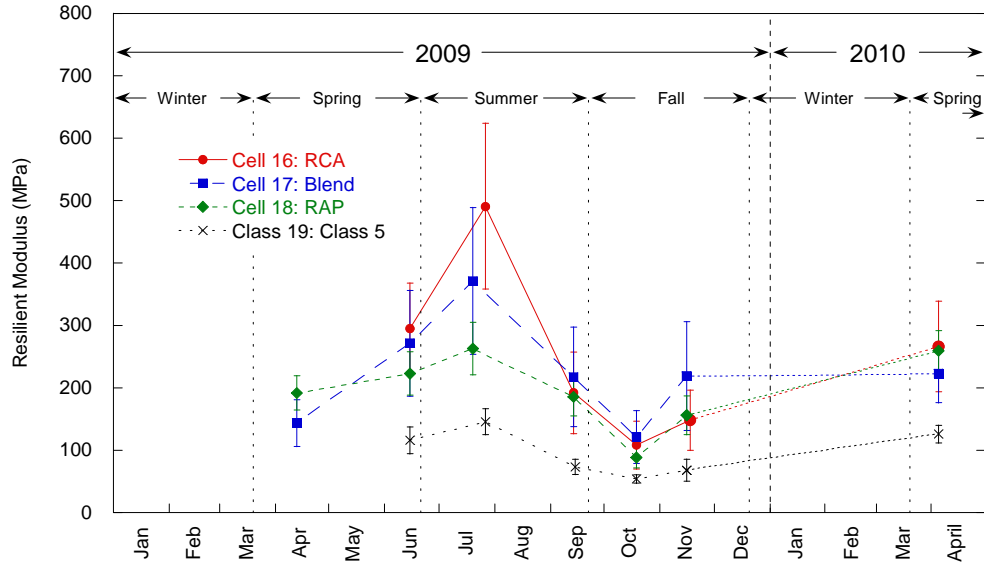


Fig.6. Resilient modulus of base course as a function of time for test cells constructed with RAP, RCA, blended RCA/Class 5, and Class 5 base course (error bars represent one standard deviation).

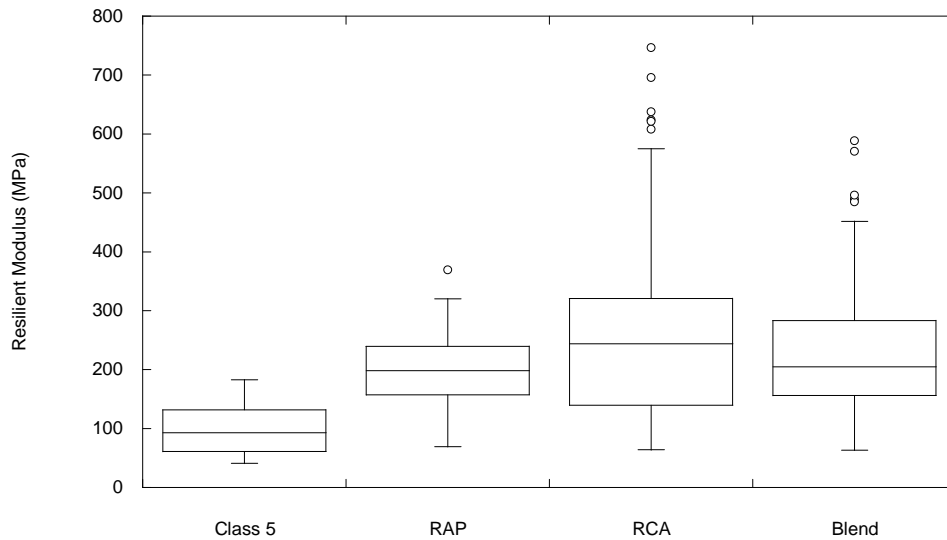


Fig.7. Comprehensive resilient modulus of all tests for cells constructed with RAP, RCA, blended RCA/Class 5, and Class 5 base course.

CONCLUSION

1. Test cells that incorporated Class 5 as a base course experienced the greatest elastic maximum deflections, followed by blended RCA/Class 5, RAP, and RCA, respectively. An increase in air temperature increases the viscosity of the overlying HMA layers and allows a greater amount of deflection to occur to the

system as a whole. Frozen subgrade contributes to a decrease in deflection during the winter months.

2. The stiffness of the HMA layers decreases during periods of increased temperature due to increased viscosity in the bituminous material. The stiffness of the base, subbase, and subgrade are relatively constant compared to that of the HMA.
3. The resilient modulus was greater at the midlane compared to the outer wheel path due to greater overall loading in these areas. The base course resilient modulus increases with a decrease in HMA modulus and decreases with an increase in HMA modulus. As the HMA becomes stiffer, the underlying base course is exposed to less translated stress and, as a result, less strain.
4. RCA and Class 5 had the highest and lowest resilient moduli, respectively. Blended RCA/Class 5 and RAP had resilient moduli that were comparable in magnitude.

BIBLIOGRAPHY

- FHWA (2008). "User Guidelines for Byproducts and Secondary Use Materials in Pavement Construction," *FHWA Report FHWA-RD-97-148*, Federal Highway Administration, McLean, Virginia.
- Guthrie, W. S., Cooley, D. and Eggett, D. L. (2007). "Effects of Reclaimed Asphalt Pavement on Mechanical Properties of Base Materials," *Transportation Research Record*, No. 2006, pp. 44-52.
- Johnson, A., Clyne, T. R., and Worel, B. J. (2009). "2008 MnROAD Phase II Construction Report," Minnesota Department of Transportation, Maplewood, Minnesota.
- Kuo S. S., Mahgoub, H. S. and Nazef, A. (2002). "Investigation of Recycled Concrete Made with Limestone Aggregate for a Base Course in Flexible Pavement", *Geomaterials*, No. 1787, pp. 99-108.
- Schaertl, G. J. (2010). "Scaling and Equivalency of Bench-Scale Tests to Field-Scale Conditions," MS Thesis, University of Wisconsin-Madison, Madison, WI.
- Son, Y. H., (2010). "Resilient Moduli of Recycled Materials," Personal Communication.